Impact of eutrophication on arsenic cycling in freshwaters

Ying Tang [a,c], Meiyi Zhang [a,*], Guoxin Sun [a], Gang Pan [a,b,*]

[a] Key Laboratory of Environmental Nanotechnology and Health Effects, Research Center for Eco-Environmental Sciences, Chinese Academy of Sciences, Beijing 100085, P. R. China

[b] Centre of Integrated Water-Energy-Food Studies (*i*WEF), School of Animal, Rural, and Environmental Sciences, Nottingham Trent University, Brackenhurst Campus, NG25 0QF, UK

[c] University of Chinese Academy of Sciences, Beijing 100049, P. R. China

Declarations of interest: none.

Corresponding authors:

[*] Gang Pan, Phone: +86-10-62849686; e-mail: gpan@rcees.ac.cn (G. Pan);

[*] Meiyi Zhang, Phone: +86-10-62943436; e-mail: myzhang@rcees.ac.cn (M.Y. Zhang)

Abstract: Many arsenic-bearing freshwaters are facing with eutrophication and consequent algae-induced anoxia/hypoxia events. However, arsenic cycling in eutrophic waters and its impact on public health are poorly understood. Laboratory simulation experiments are performed in this study to study the effect of algal blooms on the cycling of arsenic in a sediment–water–air system. We found that the anoxia induced by the degradation of algal biomass promoted an acute arsenic (mostly As(III)) release within two days from sediment to both the water and atmosphere, and the release effluxes were proportional to the algae dosage. The reduction and methylation of arsenic were enhanced at the sediment–water interface, owing to the significant increase in arsenate reductase genes (*arr*A and *ars*C), and arsenite methyltransferase genes (*ars*M) caused by increased anoxia. The analysis of synchrotron-based X-ray absorption spectroscopy indicated that the concomitantly released natural organic matter (NOM) and sulfur (S) at the sediment–water interface reduced the As(III) release to a certain extent in the later reducing period of incubation, by forming As_2S_3 (43–51%) and As(III)-Fe-NOM (28–35%). Our results highlight the needs for the *in-situ* assessment of volatile arsenic in eutrophic freshwaters with its risk to human and animal health.

Keywords: Harmful algae bloom; Arsenic volatilization; Organic matter; Arsenic metabolism functional genes; Sediment-water-air interface; X-ray absorption spectroscopy

1. Introduction

Algae blooms, affected by eutrophication and climate change, are increasing in frequency, duration, and intensity globally (Huisman et al., 2018). They threaten the ecosystem functioning of freshwaters and public health, by not only their foul odor, but also the mobilization of pollutants (e.g., arsenic, methylated Hg, Fe, methane) during algae-induced anoxia/hypoxia events (Beutel et al., 2008; Gao et al., 2012; Shi et al., 2018). Arsenic (As) is an environmentally ubiquitous and notorious carcinogen (Wang et al., 2016). Due to the continuous anthropogenic nutrient input resulting from rapid industrialization and urbanization, eutrophication is becoming an increasing challenge in many arsenic-polluted inland waters (Dirszowsky and Wilson, 2015; Gao et al., 2012; Hirata et al., 2011; Lin et al., 2016; Rahman and Hasegawa, 2012; Wei et al., 2011). In the summer when algae blooms are likely to erupt, increased total dissolved arsenic and As(III) levels have been observed in some eutrophic freshwaters, such as the mine-impacted Balmer Lake in Canada, Biwa Lake in Japan, and Dianchi Lake in China (Hasegawa et al., 2010; Martin and Pedersen, 2004; Rahman and Hasegawa, 2012; Yang et al., 2016). However, the mechanism of arsenic biogeochemical cycling in eutrophic waters, especially during algae-induced anoxia/hypoxia events remains poorly understood.

Existing studies based on field sampling and monitoring have indicated the potential correlation between algae-induced anoxia/hypoxia condition and the endogenous release of arsenic into the water column (Martin and Pedersen, 2004; Rahman and Hasegawa, 2012; Yang et al., 2016). The concentrations of total dissolved

arsenic (including As(V), As(III), methylarsonic acid (MMA), and dimethylarsinic acid (DMA(V)) released into the water column vary by several orders of magnitude, ranging from 12.2 to 8500 μg/L in different eutrophic freshwaters, depending on the total arsenic levels in sediments and the environmental chemistry (Martin and Pedersen, 2004; Rahman and Hasegawa, 2012; Yang et al., 2016). However, the maximum permissible arsenic level is 10 μg/L if freshwaters are used for drinking water (World Health Organization) or urban water supply sources (CJ/T206-2005, China) (Mohan et al., 2007). Except for the release into the water column, arsenic can also escape into the atmosphere by forming volatile arsines, such as arsine (AsH_3), monomethylarsine ($MeAsH_2$), dimethylarsine (Me_2AsH) and trimethylarsine (TMAs), through microbial activities under anaerobic conditions (Webster et al., 2016). Volatile arsenic species have been proven stable for hours during the daytime, and weeks in dark conditions in the atmosphere (Jakob et al., 2010; Mestrot et al., 2011b), thus potentially represent a serious health risks for tourists, fisherman, local residents, and wild animals (Mestrot et al., 2011b). Increasing studies have shown that arsenic volatilization from soils can be stimulated by adding exogenous natural organic matters (NOMs) such as clover, cattle manure and plant straw (Huang et al., 2012; Mestrot et al., 2011a; Mestrot et al., 2009). In eutrophic freshwater systems, senescent algae blooms serve as an exogenous NOM that is continuously deposited onto arsenic-polluted sediments (Gao et al., 2012; Hasegawa et al., 2010; Hasegawa et al., 2009; Sheng et al., 2012), which may stimulate the arsenic volatilization. However, compared to the widespread concern of various arsenic species in the water column, the release of volatile arsenic compounds in the

eutrophic freshwaters is often overlooked partly owing to the lack of satisfactory methods to measure them in the open lake field (Faust et al., 2016; Mestrot et al., 2009). Therefore, the investigation of arsenic volatilization through laboratory simulation experiments may bridge the knowledge gap in understanding the biogeochemical cycle of arsenic in eutrophic freshwaters.

The endogenous release of arsenic in freshwaters is often influenced by exogenous NOMs, however, the role of the NOMs on arsenic mobility and bioavailability is highly controversial (Langner et al., 2012). NOMs are typically recognized as affecting arsenic mobilization and bioavailability indirectly through microbial activity. The addition of NOMs (as a nutrient) can stimulate the activity of indigenous arsenic metabolism functional microbes to influence arsenic speciation, for example, from As(V) to the more mobile As(III) (Huang et al., 2012). It can also fuel the dissimilatory reducing bacteria (as an active electron donor) to drive the reduction processes of iron and sulfate in anoxic sediments (Meharg et al., 2006; Weber et al., 2010), thereby indirectly controlling arsenic mobility by the interaction of arsenic with the generated ferrous matter (Kirk et al., 2010; Xu et al., 2011) or sulfides (La Force et al., 2000; Langner et al., 2013; Moon et al., 2017). Nevertheless, NOM has been proved to be a sorbent for both As(III) and As(V) to directly control arsenic mobility (Hoffman et al., 2013). In numerous natural wetland systems and peat sediments with abundant NOMs, the enrichments of arsenic are shown not related to the presence of arsenic-bearing minerals, but through the interaction with NOMs (González et al., 2006; Langner et al., 2012, Rothwell et al., 2010). Increasing spectroscopic evidences have highlighted that

As(III)/As(V) can bind to NOMs by forming of "As-NOM" or "As-polyvalent cations-NOM" complexes, depending on the intrinsic chemical heterogeneity of the environments (Hoffmann et al., 2013; Langner et al., 2012; Langner et al., 2013). The senescent algae blooms can induce a NOM-rich anoxic sediment–water interface in eutrophic freshwaters, where interactions between NOMs and As(III) could potentially be an important mechanism for arsenic mobilization and sequestration. However, there is not enough spectroscopic evidence to assess the role of As−NOM on arsenic cycling in freshwaters suffering from algae blooms (Gao et al., 2012; Moon et al., 2017).

In this study, we investigated the biogeochemical cycling of arsenic in the microcosmic sediment–water–air system, with low algae dosage (LAD) and high algae dosage (HAD) representing the normal algae blooms level and black bloom eruption level in freshwaters, respectively. Our primary objectives are (i), to illustrate the potential risks of arsenic in aquatic and atmosphere of freshwaters undergoing eutrophication; (ii), to elucidate the mechanism of arsenic speciation and volatilization during algal biomass degradation; and (iii), to quantify the extent of arsenic binding to NOMs, sulfides and mineral oxides under different redox conditions.

2. Materials and methods

2.1 Sample collection and preparation

Surface sediment (0–10 cm) and water was sampled from Caohai (N 24°57′- 25°1′, E 102°37′-102°40′), Northeastern basin of Lake Dianchi in Kunming City, Yunnan province, China. The surface area of Lake Dianchi is 309 km^2, with an average depth

127 of 4.4 m. It is a typical arsenic-polluted lake with a total arsenic concentration of 6.55–
128 12.2 μg/L in water column and 24.5–152.9 mg/kg in surface sediments (Wei and Zhang,
129 2012; Zhang, 2013). It has been affected by annual cyanobacterial blooms since the
130 1990s (Sheng et al., 2012; Zhou et al., 2016). The characteristics of the sampled
131 sediments and water are listed in Supplementary Table S1. Algae blooms scum
132 (*Microcystis aeruginosa*) collected from the same site was freeze-dried, ground with a
133 mortar and served as the origin of NOM in the incubation experiments. Dried algal
134 biomass was chosen to exclude the arsenic metabolism origin from the fresh algae
135 themselves (Rahman and Hasegawa, 2012).

136 *2.2 Microcosm experiments*

137 Six treatments were performed with three replicates for each. (i) The control group
138 consists of sediments and lake water that represented the blank group. (ii) The LAD
139 (low algae dosage) group consists of sediments and lake water with an added 0.04 g of
140 dried algal biomass, representing the general algae level during algae blooms season
141 (Shi et al., 2018). (iii) The HAD (high algae dosage) group consists of sediments and
142 lake water with an added 0.60 g of dried algal biomass (equivalent to 5000 g fresh
143 algae/m^2), representing the black blooms condition (Han et al., 2015). (iv) The S-control
144 group consists of sterilized sediments plus lake water, represents the sterilized blank
145 group. (v) The S-HAD group, consists of sterilized sediments and lake water with an
146 added 0.60 g of sterilized dried algal biomass. (vi) The control 2 group consists of 600
147 mL of lake water with 0.60 g of added dried algal biomass, representing the arsenic
148 release potential of algal biomass itself without a sediment supply. Through a

comparison between the control, LAD, and HAD groups, we can obtain arsenic speciation and mobilization at different eutrophication-induced NOM levels. To further clarify the amount of total arsenic released from the sediments, we compared the arsenic mobilization between the control 2 and HAD groups. By comparing among the control, HAD, S-control, and S-HAD groups, the impact of microbial activity on arsenic speciation and mobilization can be evaluated. Except for control 2, all cylindrical plexiglass microcosms (Φ64 mm, length 300 mm) include 220 mL of homogenized sediments and 600 mL of lake water, with a trapping (Huang et al., 2012) of volatile arsenic installed at the top of the sealed microcosm (Supplementary Fig. S1). Details regarding the collection and quantification of volatile arsenic species are presented in Supplementary Information. In the sterilized groups, sediments, water and algal biomass were autoclaved for 20 min at 121 °C, and another 0.2% NaN_3 was added into the water to further inhibit microbial growth.

Each microcosm was stabilized for three weeks before algal biomass addition. All experiments were performed in the dark at 25 °C for 18 days. Overlying water (10 mL) was sampled at approximately 20 mm above the SWI (sediment–water interface) and filtered with 0.45 μm filter. Porewater (5 mL) was sampled with Rhizons soil moisture samplers (type MOM) from 5 mm above, and 10, 20, 30 and 40 mm below the SWI. All water samples were sampled in an anaerobic glove box at 0, 2, 4, 7, 12, 18 days after algal biomass addition and stored at -20 °C until the analyses for sulfates, DOC, Fe, and As. After each sample collection, all microcosms were replenished with the originally filtered water to compensate for the sampling losses. The mixed sediments

171 (0–20, 20–40, and > 40 mm) were sampled in an anaerobic glove box and stored at -
172 80 °C before chemical extraction, synchrotron-based X-ray absorption spectroscopy,
173 and arsenic metabolism functional gene analyses. More details of the analytical
174 methods are shown in Supplementary Information.

175 *2.3 Bulk X-ray Absorption Spectroscopy*

176 A subset of fresh sediment samples was prepared for bulk arsenic and iron K-edge
177 XAS analyses. The homogenized sediment samples were filled into Plexiglas sample
178 holders in an anaerobic glove box, sealed with Kapton® tapes and immediately stored
179 in vacuum bags before analysis. Bulk arsenic K-edge (11867 eV) and iron K-edge (7112
180 eV) XANES spectra were collected on beamlines 1W1B at the Beijing Synchrotron
181 Radiation Facility (BSRF, China). We analyzed the XANES spectra by means of linear
182 combination fitting (LCF) in the E space, over a fit range from -20 to 30 eV. Suitable
183 reference compounds (Supplementary Table S2) were identified based on the principal
184 component analysis and target-transform testing (PCT-TT) using arsenic and iron K-
185 edge XANES reference spectra. Details about the sample preparation, experimental
186 setups, measurement conditions, and data analysis can be found in Supplementary
187 Information.

188 *2.4 Arsenic metabolism functional genes analysis: DNA extraction and PCR*

189 DNA was extracted from the sediment or water samples using the mericon DNA
190 Bacteria Kit and mericon DNA Bacteria Plus Kit (Qiagen, Germany) according to the
191 manufacturer's instructions. PCR amplifications of *aio*A, *arr*A, *ars*C and *ars*M genes

192 were performed with the primers *Aro*Adeg1F/*Aro*Adeg1R and *Aro*Adeg2F/*Aro*Adeg2R,
193 AS1F/AS1R, amlt-42-f/amlt-376-r and smrc-42-f/smrc-376-r, and *ars*MF1/*ars*MR2,
194 separately (Zhang et al., 2015). The abundance of the genes was estimated using the
195 primers described above by quantitative real-time polymerase chain reaction (qPCR)
196 performed on an AB17500 Thermocycler (Applied Biosystems Inc., USA). The details
197 are shown in the Supplementary Information.

198 3. Results and discussion

199 *3.1 Algae-induced arsenic release to air*

200 Oxygen depletion by the microbial degradation of the sinking algae induced
201 hypoxia/anoxia (dissolved oxygen <1 mg/L and Eh <-150 mV) at the SWI from day 2
202 (Fig. 1A, Supplementary Fig. S4). The water of the HAD group became malodorous
203 and black owing to the generation of black ferrous sulfide precipitates (Han et al., 2015)
204 on day 4 with the anaerobic deterioration, indicating the outbreak of black blooms (Fig.
205 1a). Accompanying with the algae-induced hypoxia/anoxia, 25.4 and 100 ng of total
206 volatile arsenic (including both TMAs and AsH_3) were released into the atmosphere
207 during the 18-day incubation in the LAD and HAD groups, respectively (Fig. 1B),
208 corresponding to an average flux of 0.431 and 1.73 $\mu g/m^2 \cdot d$, respectively
209 (Supplementary Table S6). The volatilization effluxes of the total arsenic in the LAD
210 and HAD were 2 and 8 times higher than that of the control, respectively, indicating
211 that the volatilization capacity of arsenic was significantly improved under more
212 reducing conditions induced by algae degradation. Arsenic volatilization involves

arsenic reduction and methylation metabolic pathways (Challenger, 1945; Huang et al., 2012), with the metabolites of TMAs, AsH_3, $MeAsH_2$ or Me_2AsH. In this study, only TMAs and AsH_3 were detected and the predominant volatile arsenic species changed from TMAs to AsH_3, which is the most poisonous arsenic species (Faust et al., 2016), when black blooms occurred in HAD (Fig. 1B). AsH_3 production, as recognized as a fungi or methanoarchaea-induced biotransformation process under strong reducing condition (Pakulska and Czerczak, 2006; Wang et al., 2014), has also been observed in some paddies or peats with organic matter amendment (Mestrot et al., 2011a). Theoretically, AsH_3 can persist for five days under light (Pantsar-Kallio and Korpela 2000), and 19 weeks under dark conditions (Jakob et al., 2010; Mestrot et al., 2011b), thus enabling its long-distance transportation from the emission source. Therefore, algae-induced anoxia in arsenic-polluted freshwaters may pose greater health risk to the residents nearby through respiratory exposure.

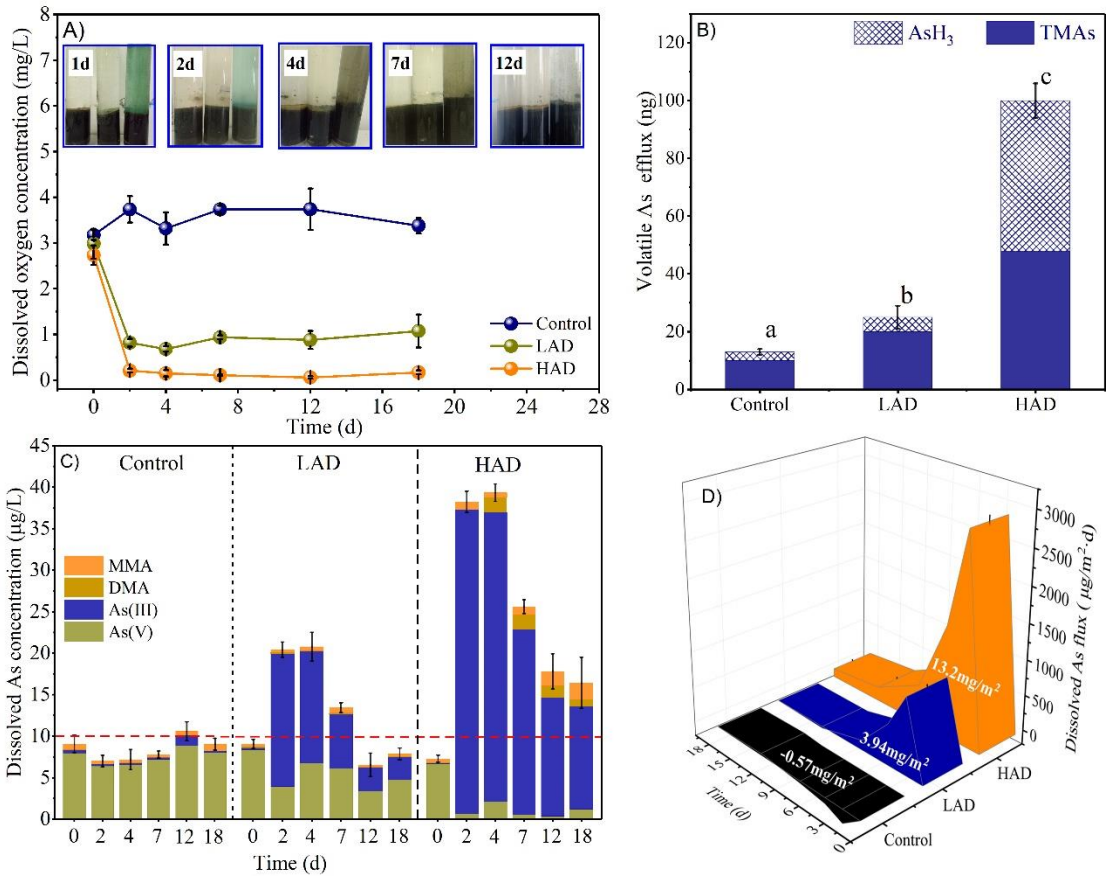

Fig. 1. Arsenic mobilization during the incubation period. *A*, Dissolve oxygen and visual changes with incubation time. Three columns in each inset indicate Control, LAD and HAD treatment, respectively; *B*, Volatile arsenic in the air. One-Way ANOVA was used to measure significant differences ($p < 0.05$) between treatments, which marked with various lowercase; *C*, Dissolved arsenic in the overlying water. The red dashed line indicates the World Health Organization drinking water limit of 10 μg/L; *D*, Dissolved arsenic flux across the sediment–water interface. The data in each bar indicates the cumulated total dissolved arsenic flux during the 18-day incubation.

3.2 Algae-induced arsenic release to water

Algae blooms degradation increased the total dissolved arsenic in the overlying water (Fig. 1C). The total dissolved arsenic in the control group remained at 7–11 μg/L throughout the experiment. In contrast, it increased following the onset of hypoxia/anoxia (Fig. 1A), peaked at day 4, followed by a gradual decrease until the end of the experiment in the LAD and HAD groups. The maximum total dissolved arsenic concentration in water in the LAD (19 μg/L) and HAD (38 μg/L) groups were 2 and 4

241 times higher than the WHO drinking water limit of 10 μg/L, respectively. Decomposed
242 algal biomass can contribute one-tenth of the increased total dissolved arsenic (3.02±
243 0.50 μg/L) in the overlying water, implying that the excess was resulted from
244 endogenous release related to algae-induced anoxia/hypoxia. This result was supported
245 by the distinct enlargement of concentration gradients for total dissolved arsenic in
246 porewater at a depth of -20–5 mm when algae were added (Supplementary Fig. S5).
247 The calculated dissolved arsenic flux across the SWI was switched from negative in the
248 control group to positive in the LAD and HAD groups over the incubation (Fig. 1D),
249 thus confirming the change from arsenic sink to source for surface sediments (0–2 cm)
250 during the microbial degradation of algae blooms. Integrating the total dissolved arsenic
251 flux data over the 18-day incubation yield a cumulated arsenic release of 3.94 mg/m^2
252 (in LAD)–13.2 mg/m^2 (in HAD) into the overlying water (Fig. 1D), corresponding to
253 an average diffusive flux of 0.219–0.733 $mg/m^2 \cdot d$ (Supplementary Table S6).

254 With the endogenous release of arsenic during algae-induced hypoxia/anoxia, the
255 predominant arsenic species converted from As(V) into As(III) (79.8–97.2%) and
256 methylated As (i.e., MMA and DMA) (2.33–11.3%) in both overlying water (Fig. 1C)
257 and surface sediments (Supplementary Fig. S6). The reduction and methylation rate of
258 arsenic increased with algae dosage, indicating that the NOM-rich anoxic condition was
259 favorable for the production of As(III) and methylated As, as observed in natural
260 eutrophic systems (Hasegawa et al., 2010; Hasegawa et al., 2009; Li et al., 2014). The
261 toxicity sequence of different arsenic species is AsH_3 > As(III) > As(V) > MMA > DMA>
262 TMAO (WH, 1981), implying that the expansion of algae blooms may enhance the

263 toxic impact of arsenic in the water column.

264 *3.3 Microbially mediated arsenic speciation*

265 Arsenic reduction and methylation processes at sediment–water–air interfaces
266 were detected after algae addition in unsterilized groups (Fig. 1B~C and Supplementary
267 Fig. S4A). However, in sterilized groups, compared to the S-control, adding high algae
268 dosage in the S-HAD group did not promote arsenic volatilization to air, arsenic
269 reduction and methylation in overlying water, and arsenic reduction in surface
270 sediments (Supplementary Fig. S7). These implied that the reduction of As(V) to As(III)
271 or AsH_3, and the methylation of As(III) to MMA, DMA or TMAs during the algae
272 decomposition was primarily a microbially mediated process, which agreed with
273 previous studies (Huang et al., 2012; Mestrot et al., 2011a). To further uncover the
274 arsenic metabolism mechanism during the microbial degradation of algal biomass, the
275 abundance of different arsenic metabolism functional genes (i.e., arsenite oxidation
276 (*aio*A), arsenate respiratory reduction (*arr*A), arsenate reduction (*ars*C), and arsenite
277 methylation (*ars*M) genes) (Suhadolnik et al., 2017; Zhang et al., 2015) in the overlying
278 water, surface sediments (0–2 cm) and deep sediments (2–4 cm) was analyzed and
279 shown in Fig. 2.

280 Significant abundance shifts of functional genes were focused on the overlying
281 water column and surface sediments (Fig. 2A and 2B, respectively), where arsenic
282 reduction and methylation mainly occurred primarily (Fig. 1C and Supplementary Fig.
283 S6). The copy number of *aio*A genes decreased significantly when algae were added,
284 indicating the inhibited growth of arsenite oxidative bacteria at the SWI. However, the

*arr*A genes notably increased from 3.10×10^6 to 9.54×10^6 copies/L in the water column (Fig. 2A), and from 2.39 ×10^6 to 4.69×10^6 copies/g in the surface sediments with increasing algae dosage (Fig. 2B), accompanied with the similar notable increase in *ars*C and *ars*M genes. These results demonstrated that the organic carbon enriched anoxic environments (Fig. 1A and Supplementary Table S7) promoted the growth of arsenate reductive bacteria and arsenite methylated bacteria, leading to more formation of arsenite, arsines and methylated arsenic at sediment–water–air interfaces (Fig. 1B and 1C).

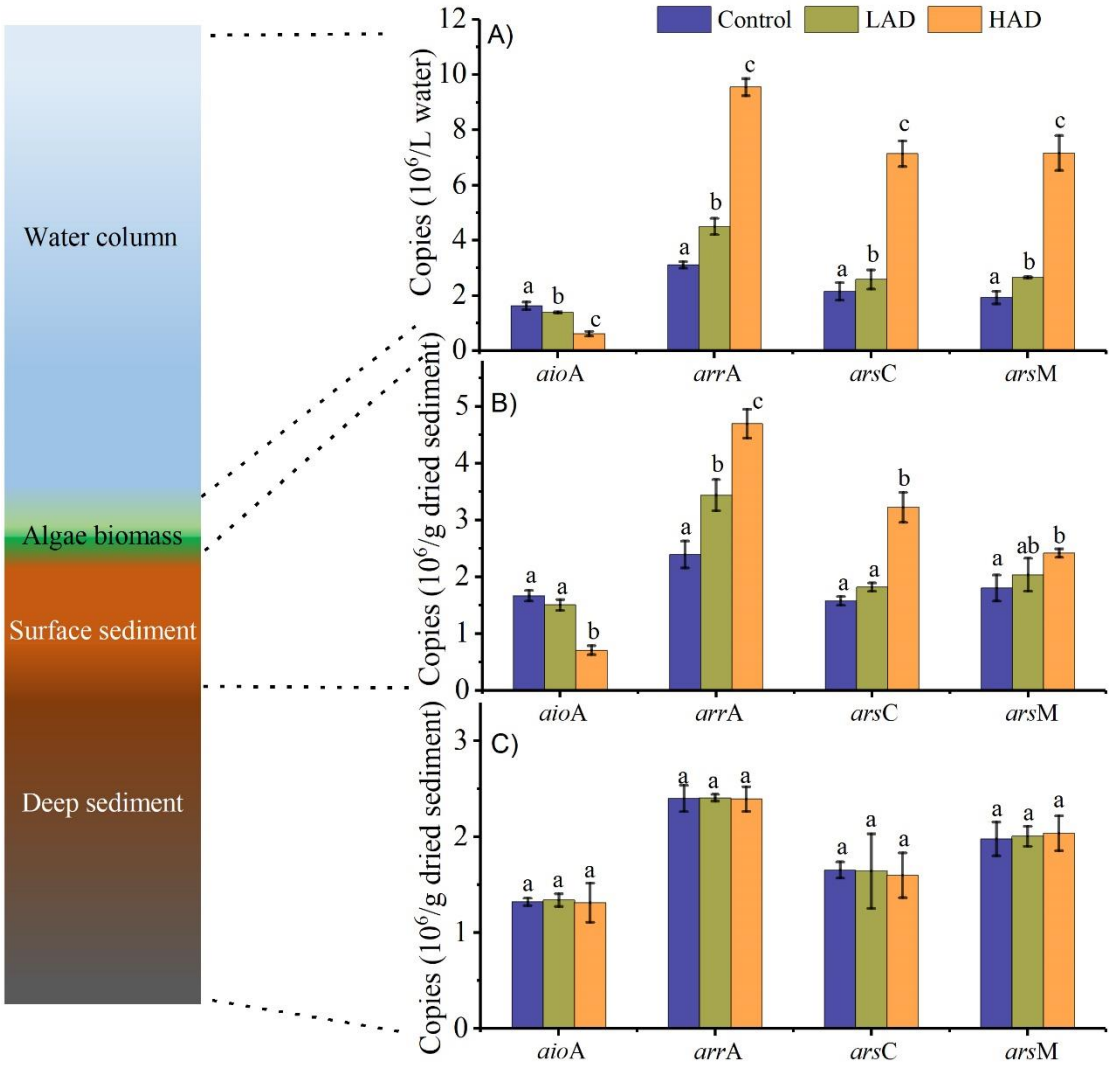

Fig. 2. Abundance of *aio*A, *arr*A, *ars*C and *ars*M genes in the overlying water (*A*), surface sediments (0–2 cm) (*B*) and deep sediments (2–4 cm) (*C*) for treatments with different algae dosage.

In each figure, One-Way ANOVA was used to measure significant differences ($p < 0.05$) between treatments, which marked with various lowercase.

3.4 Geochemically controlled arsenic release and sequestration

The endogenous release of arsenic was paralleled by the release of dissolved Fe(II) and dissolved organic carbon (DOC) from sediments. This was supported by the similar regular patterns for dissolved Fe(II) and DOC in the overlying water (Fig. 3A-B), and the increased concentration gradients of porewater dissolved Fe(II) and DOC at the depth of -20–5 mm for treatments with algal biomass compared to the control (Supplementary Fig. S5). DOC is an indicator of organic matter degradation and mineralization (Gao et al., 2012). Highly significant positive correlations ($p < 0.01$) were found between DOC and total dissolved As, DOC, and dissolved Fe(II) in water column throughout the experiment, respectively, and their correlation coefficients increased with increasing algae dosage (Fig. 3D). It clearly implied that the anaerobic degradation of algae blooms in eutrophic freshwater may develop favorable conditions (e.g., low redox at SWI (Supplementary Fig. S4) and plenty of electron donor (Postma et al., 2012)) for microbial reductive dissolution of arsenic-bearing iron oxides. This facilitated the increase in Fe(II)/TFe and As(III)/TAs in surface sediments (Supplementary Fig. S6), leading to the concurrent release of As(III) and Fe(II) into overlying water (Fig. 1C and 3B) (Bennett et al., 2012; Bose and Sharma, 2002; Roberts et al., 2009). However, although significantly positive correlations ($p < 0.05$) existed between the total dissolved As and Fe(II) in treatments with algal biomass (Fig. 3D), the correlations degraded slightly from 0.584 in the LAD group to 0.445 in the HAD group, implying that there may be alternative factors other than Fe(II) may exist that

affected the As(III) mobilization during black boom eruption.

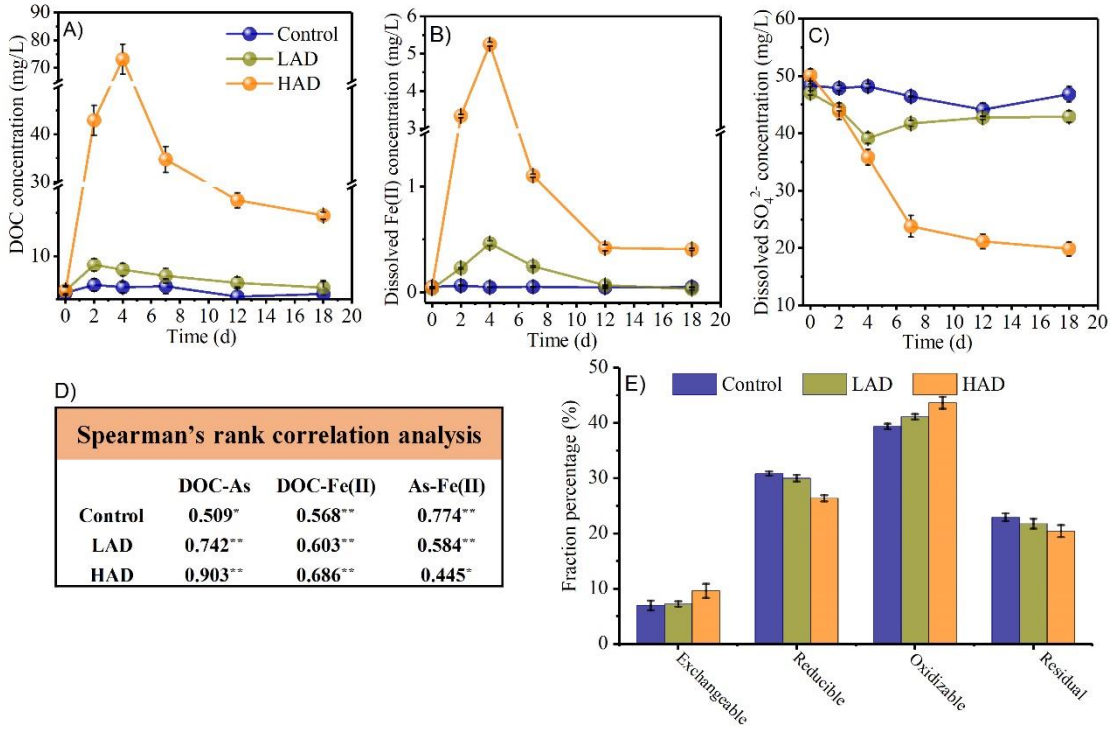

Spearman's rank correlation analysis

	DOC-As	DOC-Fe(II)	As-Fe(II)
Control	0.509*	0.568**	0.774**
LAD	0.742**	0.603**	0.584**
HAD	0.903**	0.686**	0.445*

Fig. 3. Geochemistry of arsenic release. *A-C*, DOC (dissolve organic carbon), dissolved Fe(II) and dissolved SO_4^{2-} in the overlying water; *D*, Correlation between total dissolved As, dissolved Fe(II) and DOC concentrations during the incubation period. Spearman's rank correlation analysis was done with *SPSS version 18.0*. Data for each correlation (n=24) consists of measurements taken from overlying water, -20–5 mm of porewater profiles during the 18-day incubation. Values of P <0.05 and <0.01 indicate significant (*) and highly significant (**), respectively; *E*, Arsenic fractions in surface sediments through selective extraction.

Much lower dissolved SO_4^{2-} concentrations in the overlying water and porewater profile of -20–5 mm were found in the HAD group than in both the LAD and control groups (Fig. 3C and Supplementary Fig. S5), thus verifying that the microbial sulfate reduction process was enhanced with increased anaerobic degree induced by a higher algae dosage (Han et al., 2015). The generated sulfide can immobilize As(III) by direct precipitation as arsenic sulfides, such as orpiment (As_2S_3), realgar (AsS), arsenopyrite (FeAsS) and thioarsenic species ($H_3AsO_xS_y$) (La Force et al., 2000; Langner et al., 2013; Moon et al., 2017). It can also interact with the abundant Fe(II) at anaerobic SWI (Fig.

336 3B and Fig. S6B) to form iron-sulfide precipitates (FeS or FeS_2 (pyrite)) that can
337 potentially adsorb released As(III) (Moon et al., 2017). Additionally, in this study, the
338 degradation of algae blooms induced NOM-rich anoxic environments (Fig. 3C and
339 Supplementary Table S7). This implied that NOMs can immobilize As(III), by directly
340 binding to the functional groups of NOMs (e.g., sulfhydryl group or phenolic OH group)
341 to form "NOM-As(III)" complexes, or using polyvalent metal cations (e.g., Fe) as a
342 bridge to form "NOM-polyvalent cations-As(III)" complexes (Hoffmann et al., 2013;
343 Langner et al., 2012; Langner et al., 2013; Mikutta and Kretzschmar, 2011; Sundman
344 et al., 2014). A notable increase in the oxidizable fraction of arsenic, including both
345 NOM- and S-bound arsenic in the surface sediments were found with increasing algae
346 dosage (Fig. 3E), supporting the effect of sulfide and NOM on arsenic sequestration
347 under NOM-rich anoxic environments, which can be responsible for the gradual decline
348 of total dissolved arsenic in the overlying water at the later period of the incubation
349 (Fig. 1C). To verify and quantify the interactions of arsenic with Fe, sulfides and NOMs
350 under various redox conditions, arsenic and iron K-edge X-ray absorption near-edge
351 structure (XANES) spectra analyses of surface sediments were conducted.

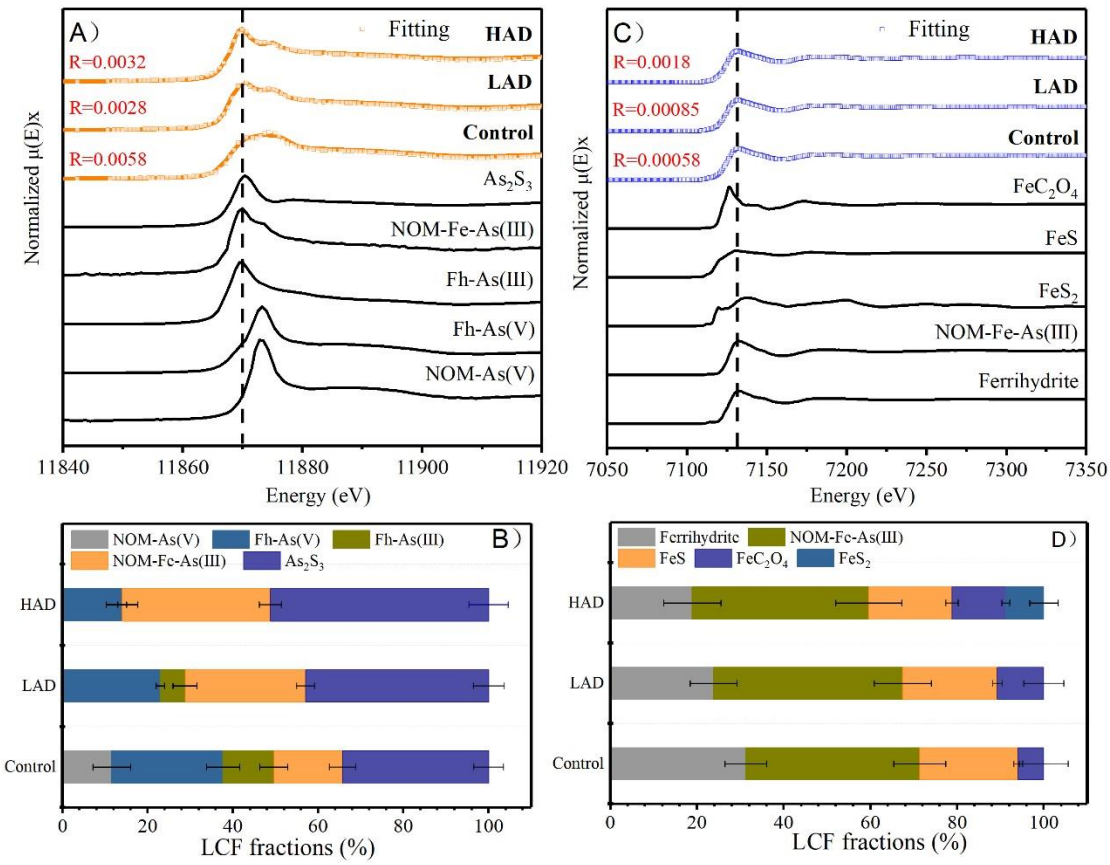

Fig. 4. Arsenic and iron speciation in the surface sediments. *A* and *C*, K-edge XANES spectra of arsenic and iron, respectively. R values show the mean square misfit between the data and the fit; *B* and *D*, speciation of arsenic and iron in surface sediments, respectively. The component sums were normalized to 100%. Fh-As(III)/As(V) indicates ferrihydrite adsorbed As(III) or As(V).

The LCF of the arsenic and iron K-edge XANES spectra of the surface sediments with reference compounds (Figs. 4A and 4C), and the corresponding fit results are summarized in Fig. 4B and 4D. With increasing algae inputs, the proportion of arsenic adsorbed to Ferrihydrite decreased from 38.0% to 14.2% (Fig. 4B), combined with Ferrihydrite fraction decreasing from 31.2% to 21.1% (Fig. 4D), respectively, confirming the primary mechanism of iron redox-controlled arsenic release in freshwaters suffering with degraded algae blooms. However, a notable increase in orpiment (As_2S_3) fraction from 34.3% to 51.2% indicated the formation of As_2S_3 under the algae-induced anaerobic condition (Fig. 4B), which even became the principal

366 As(III) sequestration during black blooms eruption. In natural systems, arsenic sulfides
367 are typically formed under high-temperature conditions such as in hot springs (O'Day
368 et al., 2004; Zhu et al., 2014). Instead, our results indicated the microbe-mediated
369 formation of As_2S_3-like minerals under sulfate-reduced anaerobic environments at
370 ambient temperature, as observed in previous studies (Bostick et al., 2004; O'Day et al.,
371 2004; Xu et al., 2011; Zhu et al., 2014). Moreover, our results also highlighted
372 particulate NOM as As(III) sequestrators by the formation of ternary complexes of
373 NOM-Fe-As(III) (Fig. 4B and 4D) during algae-induced hypoxia/anoxia. The NOM-
374 Fe-As(III) fraction can even account for approximately 35% of the solid-phase arsenic
375 speciation during black blooms eruption in freshwaters (Fig. 4B). It was formed when
376 liberated iron under strong anaerobic conditions was acted as a bridge between
377 negatively charged As(III) and the organic ligands of NOMs at the SWI, as observed in
378 arsenic-polluted deep peat layers where both iron and NOMs are enriched (Hoffmann
379 et al., 2013; Mikutta and Kretzschmar, 2011). In natural systems, polyvalent metal
380 cations can also act as bridges between other oxyanions (e.g., phosphate and selenite)
381 and organic ligands, to immobilize these oxyanions by forming similar ternary
382 complexes (Gerke, 2010; Gustafsson and Johnsson, 1994; Mikutta and Kretzschmar,
383 2011).

384 *3.5 Conceptual model for arsenic cycling*

385 In arsenic-polluted freshwaters that are coupled with eutrophication (Gao et al.,
386 2012; Rahman and Hasegawa, 2012), the mobilization of arsenic across the sediment–
387 water–air could be triggered by algae blooms (Fig. 5). The anaerobic degradation of the

senescent algae stimulated the reductive dissolution of As(V)/As(III)-bearing iron oxides in the surface sediments, causing a rapid release of Fe(II)/Fe(III) and arsenic to the water column. Algae-derived hypoxia/anoxia favored the activity of indigenous arsenate reductive bacteria (*ars*C and *arr*A genes) and arsenite methylated bacteria (*ars*M gene), thus promoting the production of As(III), MMA and DMA in the overlying water. Known as the final products of arsenic microbial reduction and methylation (Bentley and Chasteen, 2002), small amounts of AsH_3 and TMAs were formed and emitted into the atmosphere, with AsH_3 as the dominant volatile arsenic species. However, the consequent S and NOM-rich environments may serve partially as potential geochemical traps for the released As(III) in the later anoxic period of algae blooms season, by the formation of arsenic sulfides (43.0–51.2%) and NOM-Fe-As(III) (28.3–34.8%).

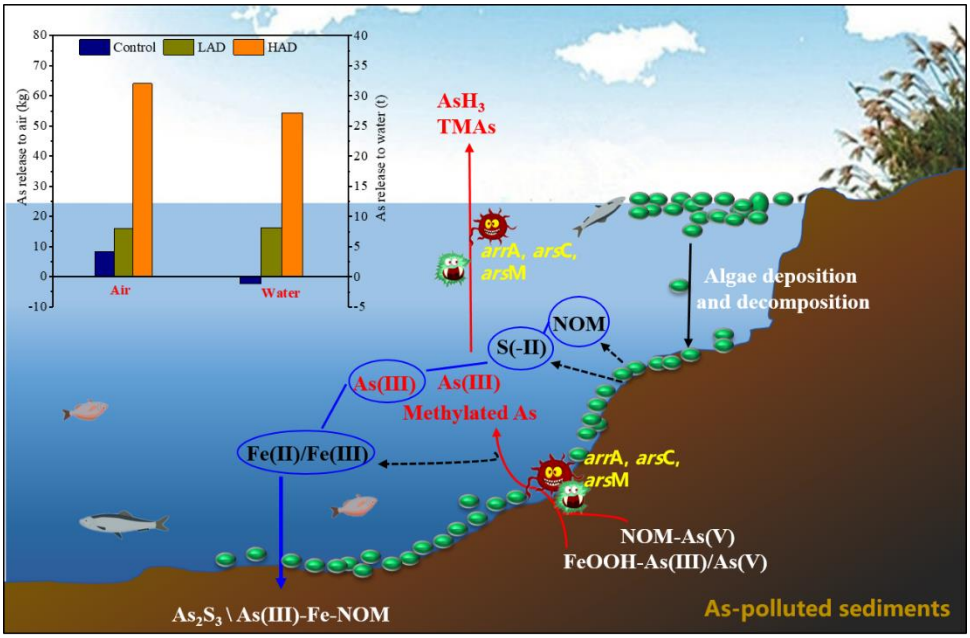

Fig. 5. A conceptual model for cycling of arsenic at the sediment-water-air interface with algae decomposition in eutrophic waters.

In natural eutrophic waters, extensive production, sinking, and subsequent

microbial decomposition of algae blooms typically lasts for months (Gao et al., 2012; Hasegawa et al., 2010; Hasegawa et al., 2009; Sheng et al., 2012), thus increasing the potential arsenic exposure risks in both water and air. Taking Lake Dianchi (309 km^2) as an example, in the normal algae blooms level, it was estimated that approximately 8.21 t of arsenic, equivalent to 3.28% of total arsenic in surface sediments, should be released into the overlying water within four months (from June to September) of algae blooms season (Sheng et al., 2012). However, during black blooms explosion, up to 27.2 t of arsenic——approximately 11% of the surface sediment arsenic capacity, can be released into water (Fig. 5, Supplementary Table S6). The released arsenic in the water column can threaten human health through direct exposure or ingestion of arsenic-accumulated aquatic organisms such as *Caridina dianchiensis* (Yang et al., 2017). Moreover, it was estimated that 16.0–64.1 kg of arsenic is likely to be volatilized during the algae blooms season per year, corresponding to 0.0065–0.026% of total arsenic present in the surface sediments (Fig. 5, Supplementary Table S6). This value is close to the volatilization rates (0.002–0.17%) for peat and paddy soils (Mestrot et al., 2011a). Arsenic biovolatilization from paddy and peat soils constitute 2–6% of the global natural arsenic emission (~46500 t/y) (Chilvers, 1987; Mestrot et al., 2011a). However, the relevant contribution estimation from eutrophic freshwaters require further clarification based on worldwide arsenic pollution status in freshwaters and its *in-situ* arsenic volatilization rules.

3.6 Environmental implications

Harmful algae blooms are currently increasing globally, and they are likely to

expand further in the coming decades owing to the continued eutrophication and worsening global warming (Huisman et al., 2018). Arsenic endogenous release to water and air induced by the degradation of senescent algae blooms, combined with the anticipated increase in release fluxes related to the intensification of eutrophication in freshwaters, highlights the need for appropriate mitigation strategies. In the short term, combating the algae-induced anoxia/hypoxia by oxygenation (Zhang et al., 2018) may be a logical and feasible method to limit arsenic endogenous release in eutrophic waters. In the long term, controlling arsenic endogenous release by the prevention of algae blooms or eutrophication in aquatic ecosystems will require extensive efforts for nutrient input control (Huisman et al., 2018).

Our results may also provide insight for arsenic dynamics in other wetlands such as paddy fields. Large areas of paddy soils in South and Southeast Asia are contaminated with arsenic (Zhao et al., 2015), where diverse exogenous organic fertilizers, such as rice straw and cattle manure, have been applied as soil amendment to obtain elevated rice yields (Huang et al., 2012). It is generally believed that arsenic accumulation in grains/straw and arsenic volatilization from rice plants and paddy soil can be promoted strongly during the decomposition of the organic fertilizers (Mestrot et al., 2011a). However, the consequent NOM- and S-rich sediments may act as traps for dissolved As(III) under a reducing condition, and therefore influence arsenic cycling in flooded paddy fields.

4. Conclusion

This study explored the effect of algal degradation on the cycling of arsenic in

eutrophic freshwaters. Algae-induced hypoxia/anoxia facilitated a rapid endogenous release of arsenic (As(III) dominant) to both overlying water and air, which may affect drinking water safety, agricultural irrigation, and recreations usage of the affected freshwaters. The reductive dissolution of arsenic-bearing iron oxides in anaerobic surface sediments was responsible for the endogenous release of As(III), although the formation of As_2S_3 and As(III)-Fe-NOM could partially ease this release process. Moreover, the accompanied reduction and methylation of arsenic was attributed to the accumulation of arsenate reductive and arsenite methylated microbe at the SWI. Future studies are required to develop efficient strategies to reduce the toxic impact of arsenic in freshwaters suffering from algae blooms.

Author contributions

G.P., M.Y.Z., G.X.S. and Y.T. conceived the experiments, which were carried out by Y.T.; G.P. provided supervision and support for Y.T.'s PhD study and revised the paper; M.Y.Z. performed synchrotron radiation data analyses and revised the paper; G.X.S. helped with the microbiological data analyses and revised the paper; Y.T. performed data interpretation and drafted the manuscript.

Acknowledgements

This work was supported by the National Key R&D Program of China (2017YFA0207204), National Natural Science Foundation of China (21377003), and Strategic Priority Research Program of the Chinese Academy of Sciences (XDA09030203). We thank Y. G. Zhu and Y. Zhao for their substantial help with

microbiological data analysis. We thank BSRF for providing the beam time and L.R. Zheng, P.F. An and K. Tang for help in XANES data collection and analysis.

Appendix A. Supplementary data

Supplementary data related to this article can be found at the online version of the paper.

References

Bennett, W.W., Teasdale, P.R., Panther, J.G., Welsh, D.T., Zhao, H. and Jolley, D.F., 2012. Investigating arsenic speciation and mobilization in sediments with DGT and DET: a mesocosm evaluation of oxic-anoxic transitions. Environ. Sci. Technol. 46(7), 3981-3989.

Bentley, R. and Chasteen, T.G., 2002. Microbial Methylation of Metalloids: Arsenic, Antimony, and Bismuth. Microbiol. Mol. Biol. Rev. 66(2), 250-271.

Beutel, M.W., Leonard, T.M., Dent, S.R. and Moore, B.C., 2008. Effects of aerobic and anaerobic conditions on P, N, Fe, Mn, and Hg accumulation in waters overlaying profundal sediments of an oligo-mesotrophic lake. Water Res. 42(8), 1953-1962.

Bose, P. and Sharma, A., 2002. Role of iron in controlling speciation and mobilization of arsenic in subsurface environment. Water Res. 36(19), 4916-4926.

Bostick, B.C., Chen, C. and Fendorf, S., 2004. Arsenite retention mechanisms within estuarine sediments of Pescadero, CA. Environ. Sci. Technol. 38(12), 3299-3304.

Challenger, F., 1945. Biological Methylation. Chemical Reviews 36(3), 315-361.

Chilvers D C , P.P.J., 1987. Global cycling of arsenic. Lead, mercury, cadmium, and arsenic in the environment, John Wiley & Sons Press, New York.

Dirszowsky, R.W. and Wilson, K.M., 2015. Biogeochemical evidence of eutrophication and metal contamination of Frame Lake, City of Yellowknife, Northwest Territories, Canada. Environ. Earth Sci. 75(1), 1-13.

Faust, J.A., Junninen, H., Ehn, M., Chen, X., Ruusuvuori, K., Kieloaho, A.-J., Bäck, J., Ojala, A., Jokinen, T., Worsnop, D.R., Kulmala, M. and Petäjä, T., 2016. Real-time detection of arsenic cations from ambient air in boreal forest and lake environments. Environ. Sci. Tech. Let. 3(2), 42-46.

Gao, Y., Leermakers, M., Pede, A., Magnier, A., Sabbe, K., Lourino Cabana, B., Billon, G., Baeyens, W. and Gillan, D.C., 2012. Response of diffusive equilibrium in thin films (DET) and diffusive gradients in thin films (DGT) trace metal profiles in sediments to phytodetritus mineralisation. Environ. Chem. 9(1), 41-47.

Gerke, J., 2010. Humic (Organic Matter)-Al(Fe)-Phosphate Complexes: An underestimated phosphate form in soils and source of plant-available phosphate. Soil Sci. 175(9), 417-425.

González A, Z.I., Krachler, M., Cheburkin, A.K. and Shotyk, W., 2006. Spatial distribution of natural enrichments of arsenic, selenium, and uranium in a minerotrophic peatland, Gola di Lago, Canton Ticino, Switzerland. Environ. Sci. Technol. 40(21), 6568-6574.

Gustafsson, J.P. and Johnsson, L., 1994. The association between selenium and humic substances

in forested ecosystems—laboratory evidence. Appl. Organomet. Chem. 8(2), 141-147.

Han, C., Ding, S., Yao, L., Shen, Q., Zhu, C., Wang, Y. and Xu, D., 2015. Dynamics of phosphorus–iron–sulfur at the sediment–water interface influenced by algae blooms decomposition. J. Hazard. Mater. 300, 329-337.

Hasegawa, H., Rahman, M.A., Kitahara, K., Itaya, Y., Maki, T. and Ueda, K., 2010. Seasonal changes of arsenic speciation in lake waters in relation to eutrophication. Sci. Total Environ. 408(7), 1684-1690.

Hasegawa, H., Rahman, M.A., Matsuda, T., Kitahara, T., Maki, T. and Ueda, K., 2009. Effect of eutrophication on the distribution of arsenic species in eutrophic and mesotrophic lakes. Sci. Total Environ. 407(4), 1418-1425.

Hirata, S.H., Hayase, D., Eguchi, A., Itai, T., Nomiyama, K., Isobe, T., Agusa, T., Ishikawa, T., Kumagai, M. and Tanabe, S., 2011. Arsenic and Mn levels in Isaza (Gymnogobius isaza) during the mass mortality event in Lake Biwa, Japan. Environ. Pollut. 159(10), 2789-2796.

Hoffmann, M., Mikutta, C. and Kretzschmar, R., 2013. Arsenite binding to natural organic matter: spectroscopic evidence for ligand exchange and ternary complex formation. Environ. Sci. Technol. 47(21), 12165-12173.

Huang, H., Jia, Y., Sun, G.X. and Zhu, Y.G., 2012. Arsenic speciation and volatilization from flooded paddy soils amended with different organic matters. Environ. Sci. Technol. 46(4), 2163-2168.

Huisman, J., Codd, G.A., Paerl, H.W., Ibelings, B.W., Verspagen, J.M.H. and Visser, P.M., 2018. Cyanobacterial blooms. Nat. Rev. Microbiol.

Jakob, R., Roth, A., Haas, K., Krupp, E.M., Raab, A., Smichowski, P., Gomez, D. and Feldmann, J., 2010. Atmospheric stability of arsines and the determination of their oxidative products in atmospheric aerosols (PM_{10}): evidence of the widespread phenomena of biovolatilization of arsenic. J. Environ. Monitor. 12(2), 409-416.

Kirk, M.F., Roden, E.E., Crossey, L.J., Brealey, A.J. and Spilde, M.N., 2010. Experimental analysis of arsenic precipitation during microbial sulfate and iron reduction in model aquifer sediment reactors. Geochim. Cosmochim. Acta 74(9), 2538-2555.

La Force, M.J., Hansel, C.M. and Fendorf, S., 2000. Arsenic Speciation, Seasonal transformations, and co-distribution with iron in a mine waste-influenced palustrine emergent wetland. Environ. Sci. Technol. 34(18), 3937-3943.

Langner, P., Mikutta, C. and Kretzschmar, R., 2012. Arsenic sequestration by organic sulphur in peat. Nat. Geosci. 5(1), 66-73.

Langner, P., Mikutta, C., Suess, E., Marcus, M.A. and Kretzschmar, R., 2013. Spatial distribution and speciation of arsenic in peat studied with microfocused X-ray fluorescence spectrometry and X-ray absorption spectroscopy. Environ. Sci. Technol. 47(17), 9706-9714.

Li, L., Ren, J.-L., Yan, Z., Liu, S.-M., Wu, Y., Zhou, F., Liu, C.G. and Zhang, J., 2014. Behavior of arsenic in the coastal area of the Changjiang (Yangtze River) Estuary: Influences of water mass mixing, the spring bloom and hypoxia. Cont. Shelf Res. 80, 67-78.

Lin, Q., Liu, E., Zhang, E., Li, K. and Shen, J., 2016. Spatial distribution, contamination and ecological risk assessment of heavy metals in surface sediments of Erhai Lake, a large eutrophic plateau lake in southwest China. CATENA 145, 193-203.

Martin, A.J. and Pedersen, T.F., 2004. Alteration to lake trophic status as a means to control arsenic mobility in a mine-impacted lake. Water Res. 38(20), 4415-4423.

Meharg, A.A., Scrimgeour, C., Hossain, S.A., Fuller, K., Cruickshank, K., Williams, P.N. and Kinniburgh, D.G., 2006. Codeposition of organic carbon and arsenic in Bengal Delta Aquifers. Environ. Sci. Technol. 40(16), 4928-4935.

Mestrot, A., Feldmann, J., Krupp, E.M., Hossain, M.S., Roman-Ross, G. and Meharg, A.A., 2011a. Field fluxes and speciation of arsines emanating from soils. Environ. Sci. Technol. 45(5), 1798-1804.

Mestrot, A., Merle, J.K., Broglia, A., Feldmann, J. and Krupp, E.M., 2011b. Atmospheric stability of arsine and methylarsines. Environ. Sci. Technol. 45(9), 4010-4015.

Mestrot, A., Uroic, M.K., Plantevin, T., Islam, M.R., Krupp, E.M., Feldmann, J. and Meharg, A.A., 2009. Quantitative and qualitative trapping of arsines deployed to assess loss of volatile arsenic from paddy soil. Environ. Sci. Technol. 43(21), 8270-8275.

Mikutta, C. and Kretzschmar, R., 2011. Spectroscopic evidence for ternary complex formation between arsenate and ferric iron complexes of humic substances. Environ. Sci. Technol. 45(22), 9550-9557.

Mohan, D., Pittman Jr., C.U., 2007. Arsenic removal from water/wastewater using adsorbents – a critical review. J. Hazard. Mater. 142, 1–53.

Moon, H.S., Kim, B.A., Hyun, S.P., Lee, Y.H. and Shin, D., 2017. Effect of the redox dynamics on microbial-mediated As transformation coupled with Fe and S in flow-through sediment columns. J. Hazard. Mater. 329, 280-289.

O'Day, P.A., Vlassopoulos, D., Root, R. and Rivera, N., 2004.The influence of sulfur and iron on dissolved arsenic concentrations in the shallow subsurface under changing redox conditions. P. Natl. Acad. Sci. USA 101(38), 13703-13708.

Pakulska, D. and Czerczak, S., 2006. Hazardous effects of arsine: a short review, p. 36.

Pantsar-Kallio, M. and Korpela, A., 2000. Analysis of gaseous arsenic species and stability studies of arsine and trimethylarsine by gas chromatography-mass spectrometry. Anal. Chim. Acta 410(1), 65-70.

Postma, D., Larsen, F., Thai, N.T., Trang, P.T.K., Jakobsen, R., Nhan, P.Q., Long, T.V., Viet, P.H. and Murray, A.S., 2012. Groundwater arsenic concentrations in Vietnam controlled by sediment age. Nat. Geosci. 5(9), 656-661.

Rahman, M.A. and Hasegawa, H., 2012. Arsenic in freshwater systems: Influence of eutrophication on occurrence, distribution, speciation, and bioaccumulation. Appl. Geochem. 27(1), 304-314.

Roberts, L.C., Hug, S.J., Dittmar, J., Voegelin, A., Kretzschmar, R., Wehrli, B., Cirpka, O.A., Saha, G.C., Ali, M.A. and Badruzzaman, A.B.M., 2009. Arsenic release from paddy soils during monsoon flooding. Nat. Geosci. 3(1), 53-59.

Rothwell, J.J., Taylor, K.G., Chenery, S.R.N., Cundy, A.B., Evans, M.G. and Allottt, T.E.H., 2010. Storage and behavior of As, Sb, Pb, and Cu in ombrotrophic peat bogs under contrasting water table conditions. Environ. Sci. Technol. 44(22), 8497-8502.

Sheng, H., Liu, H., Wang, C., Guo, H., Liu, Y. and Yang, Y., 2012. Analysis of cyanobacteria bloom in the Waihai part of Dianchi Lake, China. Ecol. Inform. 10 (Supplement C), 37-48.

Shi, W., Pan, G., Chen, Q., Song, L.-R., Zhu, L. and Ji, X., 2018. Hypoxia remediation and methane emission manipulation using surface oxygen nanobubbles. Environ. Sci. Technol. 52(15), 8712-8717.

Suhadolnik, M.L.S., Salgado, A.P.C., Scholte, L.L.S., Bleicher, L., Costa, P.S., Reis, M.P., Dias, M.F., Ávila, M.P., Barbosa, F.A.R., Chartone-Souza, E. and Nascimento, A.M.A., 2017. Novel

arsenic-transforming bacteria and the diversity of their arsenic-related genes and enzymes arising from arsenic-polluted freshwater sediment. Sci. Rep. 7(1), 11231.

Sundman, A., Karlsson, T., Sjöberg, S. and Persson, P., 2014. Complexation and precipitation reactions in the ternary As(V)–Fe(III)–OM (organic matter) system. Geochim. Cosmochim. Acta 145, 297-314.

Wang, C., Yao, Y., Wang, P., Hou, J., Qian, J., Yuan, Y. and Fan, X., 2016. In situ high-resolution evaluation of labile arsenic and mercury in sediment of a large shallow lake. Sci. Total Environ. 541, 83-91.

Wang, P., Sun, G., Jia, Y., Meharg, A.A. and Zhu, Y., 2014. A review on completing arsenic biogeochemical cycle: Microbial volatilization of arsines in environment. J. Environ. Sci. 26(2), 371-381.

Weber, F.A., Hofacker, A.F., Voegelin, A. and Kretzschmar, R., 2010. Temperature dependence and coupling of iron and arsenic reduction and release during flooding of a contaminated soil. Environ. Sci. Technol. 44(1), 116-122.

Webster, T.M., Reddy, R.R., Tan, J.Y., Van Nostrand, J.D., Zhou, J., Hayes, K.F. and Raskin, L., 2016. Anaerobic disposal of arsenic-bearing wastes results in low microbially mediated arsenic volatilization. Environ. Sci. Technol. 50(20), 10951-10959.

Wei, C. and Zhang, N., 2012. Arsenic variation in two basins of Lake Dianchi. Bull Environ. Contam. Toxicol. 88(4), 605-610.

Wei, C.Y., Zhang, N. and Yang, L.S., 2011. The fluctuation of arsenic levels in Lake Taihu. Biol. Trace Elem. Res. 143(3), 1310-1318.

WH, O. (1981) Environmental health criteria: arsenic, World Health Organization, Geneva.

Xu, L., Zhao, Z., Wang, S., Pan, R. and Jia, Y., 2011. Transformation of arsenic in offshore sediment under the impact of anaerobic microbial activities. Water Res. 45(20), 6781-6788.

Yang, F., Geng, D., Wei, C., Ji, H. and Xu, H., 2016. Distribution of arsenic between the particulate and aqueous phases in surface water from three freshwater lakes in China. Environ. Sci. Pollut. Res. 23(8), 7452-7461.

Yang, F., Zhang, N., Wei, C., Liu, J. and Xie, S., 2017. Arsenic speciation in organisms from two large shallow freshwater lakes in China. Bull Environ. Contam. Toxicol. 98(2), 226-233.

Zhang, H., Lyu, T., Bi, L., Tempero, G., Hamilton, D.P. and Pan, G., 2018. Combating hypoxia/anoxia at sediment-water interfaces: A preliminary study of oxygen nanobubble modified clay materials. Sci. Total Environ. 637-638, 550-560.

Zhang, N., 2013. Occurrence, distribution, migration and bioaccumulation of arsenic in large shallow freshwater lake, University of Chinese Academy of Sciences, Beijing. (Chinese)

Zhang, S.Y., Zhao, F.J., Sun, G.X., Su, J.Q., Yang, X.R., Li, H. and Zhu, Y.G., 2015. Diversity and abundance of arsenic biotransformation genes in paddy soils from southern China. Environ. Sci. Technol. 49(7), 4138-4146.

Zhao, F.J., Ma, Y., Zhu, Y.G., Tang, Z. and McGrath, S.P., 2015. Soil contamination in China: current status and mitigation strategies. Environ. Sci. Technol. 49(2), 750-759.

Zhou, Q., Zhang, Y., Lin, D., Shan, K., Luo, Y., Zhao, L., Tan, Z. and Song, L., 2016. The relationships of meteorological factors and nutrient levels with phytoplankton biomass in a shallow eutrophic lake dominated by cyanobacteria, Lake Dianchi from 1991 to 2013. Environ. Sci. Pollut. Res. 23(15), 15616-15626.

Zhu, Y.G., Yoshinaga, M., Zhao, F.J. and Rosen, B.P., 2014. Earth abides arsenic biotransformations.

638 Annu. Rev. Earth Pl. Sc. 42(1), 443-467.